21. THE COSMOLOGICAL PARAMETERS

Updated September 2007, by O. Lahav (University College London) and A.R. Liddle (University of Sussex).

21.1. Parametrizing the Universe

Rapid advances in observational cosmology are leading to the establishment of the first precision cosmological model, with many of the key cosmological parameters determined to one or two significant figure accuracy. Particularly prominent are measurements of cosmic microwave anisotropies, led by the three-year results from the Wilkinson Microwave Anisotropy Probe (WMAP) [1,2]. However the most accurate model of the Universe requires consideration of a wide range of different types of observation, with complementary probes providing consistency checks, lifting parameter degeneracies, and enabling the strongest constraints to be placed.

The term 'cosmological parameters' is forever increasing in its scope, and nowadays includes the parametrization of some functions, as well as simple numbers describing properties of the Universe. The original usage referred to the parameters describing the global dynamics of the Universe, such as its expansion rate and curvature. Also now of great interest is how the matter budget of the Universe is built up from its constituents: baryons, photons, neutrinos, dark matter, and dark energy. We need to describe the nature of perturbations in the Universe, through global statistical descriptions such as the matter and radiation power spectra. There may also be parameters describing the physical state of the Universe, such as the ionization fraction as a function of time during the era since decoupling. Typical comparisons of cosmological models with observational data now feature between five and ten parameters.

21.1.1. *The global description of the Universe* :

Ordinarily, the Universe is taken to be a perturbed Robertson–Walker space-time with dynamics governed by Einstein's equations. This is described in detail by Olive and Peacock in this volume. Using the density parameters Ω_i for the various matter species and Ω_Λ for the cosmological constant, the Friedmann equation can be written

$$\sum_i \Omega_i + \Omega_\Lambda = \frac{k}{R^2 H^2}\,, \tag{21.1}$$

where the sum is over all the different species of matter in the Universe. This equation applies at any epoch, but later in this article we will use the symbols Ω_i and Ω_Λ to refer to the present values. A typical collection would be baryons, photons, neutrinos, and dark matter (given charge neutrality, the electron density is guaranteed to be too small to be worth considering separately).

The complete present state of the homogeneous Universe can be described by giving the present values of all the density parameters and the present Hubble parameter h. These also allow us to track the history of the Universe back in time, at least until an epoch where interactions allow interchanges between the densities of the different species, which is believed to have last happened at neutrino decoupling shortly before nucleosynthesis. To probe further back into the Universe's history requires assumptions about particle interactions, and perhaps about the nature of physical laws themselves.

21.1.2. ***Neutrinos*** :

The standard neutrino sector has three flavors. For neutrinos of mass in the range $5 \times 10^{-4}\,\mathrm{eV}$ to $1\,\mathrm{MeV}$, the density parameter in neutrinos is predicted to be

$$\Omega_\nu h^2 = \frac{\sum m_\nu}{93\,\mathrm{eV}}\,, \tag{21.2}$$

where the sum is over all families with mass in that range (higher masses need a more sophisticated calculation). We use units with $c = 1$ throughout. Results on atmospheric and solar neutrino oscillations [3] imply non-zero mass-squared differences between the three neutrino flavors. These oscillation experiments cannot tell us the absolute neutrino masses, but within the simple assumption of a mass hierarchy suggest a lower limit of $\Omega_\nu \approx 0.001$ on the neutrino mass density parameter.

For a total mass as small as $0.1\,\mathrm{eV}$, this could have a potentially observable effect on the formation of structure, as neutrino free-streaming damps the growth of perturbations. Present cosmological observations have shown no convincing evidence of any effects from either neutrino masses or an otherwise non-standard neutrino sector, and impose quite stringent limits, which we summarize in Section 21.3.4. Consequently, the standard assumption at present is that the masses are too small to have a significant cosmological impact, but this may change in the near future.

The cosmological effect of neutrinos can also be modified if the neutrinos have decay channels, or if there is a large asymmetry in the lepton sector manifested as a different number density of neutrinos versus anti-neutrinos. This latter effect would need to be of order unity to be significant, rather than the 10^{-9} seen in the baryon sector, which may be in conflict with nucleosynthesis [4].

21.1.3. ***Inflation and perturbations*** :

A complete model of the Universe should include a description of deviations from homogeneity, at least in a statistical way. Indeed, some of the most powerful probes of the parameters described above come from the evolution of perturbations, so their study is naturally intertwined in the determination of cosmological parameters.

There are many different notations used to describe the perturbations, both in terms of the quantity used to describe the perturbations and the definition of the statistical measure. We use the dimensionless power spectrum Δ^2 as defined in Olive and Peacock (also denoted $\mathcal{P}$ in some of the literature). If the perturbations obey Gaussian statistics, the power spectrum provides a complete description of their properties.

From a theoretical perspective, a useful quantity to describe the perturbations is the curvature perturbation $\mathcal{R}$, which measures the spatial curvature of a comoving slicing of the space-time. A case of particular interest is the Harrison–Zel'dovich spectrum, which corresponds to a constant spectrum $\Delta^2_{\mathcal{R}}$. More generally, one can approximate the spectrum by a power-law, writing

$$\Delta^2_{\mathcal{R}}(k) = \Delta^2_{\mathcal{R}}(k_*) \left[\frac{k}{k_*}\right]^{n-1}\,, \tag{21.3}$$

where n is known as the spectral index, always defined so that $n = 1$ for the Harrison–Zel'dovich spectrum, and k_* is an arbitrarily chosen scale. The initial spectrum, defined at some early epoch of the Universe's history, is usually taken to have a simple form such as this power-law, and we will see that observations require n close to one, which corresponds to the perturbations in the curvature being independent of scale. Subsequent evolution will modify the spectrum from its initial form.

The simplest viable mechanism for generating the observed perturbations is the inflationary cosmology, which posits a period of accelerated expansion in the Universe's early stages [5]. It is a useful working hypothesis that this is the sole mechanism for generating perturbations. Commonly, it is further assumed to be the simplest class of inflationary model, where the dynamics are equivalent to that of a single scalar field ϕ slowly rolling on a potential $V(\phi)$. One aim of cosmology is to verify that this simple picture can match observations, and to determine the properties of $V(\phi)$ from the observational data.

Inflation generates perturbations through the amplification of quantum fluctuations, which are stretched to astrophysical scales by the rapid expansion. The simplest models generate two types, density perturbations which come from fluctuations in the scalar field and its corresponding scalar metric perturbation, and gravitational waves which are tensor metric fluctuations. The former experience gravitational instability and lead to structure formation, while the latter can influence the cosmic microwave background anisotropies. Defining slow-roll parameters, with primes indicating derivatives with respect to the scalar field, as

$$\epsilon = \frac{m_{\rm Pl}^2}{16\pi}\left(\frac{V'}{V}\right)^2 \quad ; \quad \eta = \frac{m_{\rm Pl}^2}{8\pi}\frac{V''}{V}\,, \tag{21.4}$$

which should satisfy $\epsilon, |\eta| \ll 1$, the spectra can be computed using the slow-roll approximation as

$$\begin{aligned} \Delta^2_{\mathcal{R}}(k) &\simeq \frac{8}{3m_{\rm Pl}^4}\frac{V}{\epsilon}\bigg|_{k=aH}\,; \\ \Delta^2_{\rm grav}(k) &\simeq \frac{128}{3m_{\rm Pl}^4}V\bigg|_{k=aH}\,. \end{aligned} \tag{21.5}$$

In each case, the expressions on the right-hand side are to be evaluated when the scale k is equal to the Hubble radius during inflation. The symbol '$\simeq$' indicates use of the slow-roll approximation, which is expected to be accurate to a few percent or better.

From these expressions, we can compute the spectral indices

$$n \simeq 1 - 6\epsilon + 2\eta \quad ; \quad n_{\rm grav} \simeq -2\epsilon\,. \tag{21.6}$$

Another useful quantity is the ratio of the two spectra, defined by

$$r \equiv \frac{\Delta^2_{\rm grav}(k_*)}{\Delta^2_{\mathcal{R}}(k_*)}\,. \tag{21.7}$$

The literature contains a number of definitions of r; this convention matches that of recent versions of CMBFAST [6] and that used by WMAP [8], while definitions based on the relative effect on the microwave background anisotropies typically differ by tens of percent. We have

$$r \simeq 16\epsilon \simeq -8n_{\rm grav}\,, \tag{21.8}$$

which is known as the consistency equation.

In general, one could consider corrections to the power-law approximation, which we discuss later. However, for now we make the working assumption that the spectra can be approximated by power laws. The consistency equation shows that r and $n_{\rm grav}$ are not independent parameters, and so the simplest inflation models give initial conditions described by three parameters, usually taken as $\Delta^2_{\mathcal{R}}$, n, and r, all to be evaluated at some scale k_*, usually the 'statistical centre' of the range explored by the data. Alternatively, one could use the parametrization V, ϵ, and η, all evaluated at a point on the putative inflationary potential.

After the perturbations are created in the early Universe, they undergo a complex evolution up until the time they are observed in the present Universe. While the perturbations are small, this can be accurately followed using a linear theory numerical code such as CMBFAST [6]. This works right up to the present for the cosmic microwave background, but for density perturbations on small scales non-linear evolution is important and can be addressed by a variety of semi-analytical and numerical techniques. However the analysis is made, the outcome of the evolution is in principle determined by the cosmological model, and by the parameters describing the initial perturbations, and hence can be used to determine them.

Of particular interest are cosmic microwave background anisotropies. Both the total intensity and two independent polarization modes are predicted to have anisotropies. These can be described by the radiation angular power spectra C_ℓ as defined in the article of Scott and Smoot in this volume, and again provide a complete description if the density perturbations are Gaussian.

21.1.4. *The standard cosmological model* :

We now have most of the ingredients in place to describe the cosmological model. Beyond those of the previous subsections, there are two parameters which are essential — a measure of the ionization state of the Universe and the galaxy bias parameter. The Universe is known to be highly ionized at low redshifts (otherwise radiation from distant quasars would be heavily absorbed in the ultra-violet), and the ionized electrons can scatter microwave photons altering the pattern of observed anisotropies. The most convenient parameter to describe this is the optical depth to scattering τ (*i.e.*, the probability that a given photon scatters once); in the approximation of instantaneous and complete re-ionization, this could equivalently be described by the redshift of re-ionization $z_{\rm ion}$. The bias parameter, described fully later, is needed to relate the observed galaxy power spectrum to the predicted dark matter power spectrum. The basic set of cosmological parameters is therefore as shown in Table 21.1. The spatial curvature does not appear in the list, because it can be determined from the other parameters using

Eq. (21.1). The total present matter density $\Omega_{\rm m} = \Omega_{\rm dm} + \Omega_{\rm b}$ is usually used in place of the dark matter density.

Table 21.1: The basic set of cosmological parameters. We give values (with some additional rounding) as obtained using a fit of a ΛCDM cosmology with a power-law initial spectrum to WMAP3 data alone [2]. Tensors are assumed zero except in quoting a limit on them. We cannot stress too much that the exact values and uncertainties depend on both the precise datasets used and the choice of parameters allowed to vary, and the effects of varying some assumptions will be shown later in Table 21.2. Limits on the cosmological constant depend on whether the Universe is assumed flat. The density perturbation amplitude is specified by the derived parameter σ_8. Uncertainties are one-sigma/68% confidence unless otherwise stated.

Parameter	Symbol	Value
Hubble parameter	h	0.73 ± 0.03
Total matter density	$\Omega_{\rm m}$	$\Omega_{\rm m}h^2 = 0.128 \pm 0.008$
Baryon density	$\Omega_{\rm b}$	$\Omega_{\rm b}h^2 = 0.0223 \pm 0.0007$
Cosmological constant	Ω_Λ	See Ref. 2
Radiation density	$\Omega_{\rm r}$	$\Omega_{\rm r}h^2 = 2.47 \times 10^{-5}$
Neutrino density	Ω_ν	See Sec. 21.1.2
Density perturbation amplitude	σ_8	0.76 ± 0.05
Density perturbation spectral index	n	$n = 0.958 \pm 0.016$
Tensor to scalar ratio	r	$r < 0.65$ (95% conf)
Ionization optical depth	τ	$\tau = 0.089 \pm 0.030$
Bias parameter	b	See Sec. 21.3.4

Most attention to date has been on parameter estimation, where a set of parameters is chosen by hand and the aim is to constrain them. Interest has been growing towards the higher-level inference problem of model selection, which compares different choices of parameter sets. Bayesian inference offers an attractive framework for cosmological model selection, setting a tension between model complexity and ability to fit the data.

As described in Sec. 21.4, models based on these eleven parameters are able to give a good fit to the complete set of high-quality data available at present, and indeed some simplification is possible. Observations are consistent with spatial flatness, and indeed the inflation models so far described automatically generate negligible spatial curvature, so we can set $k = 0$; the density parameters then must sum to one, and so one can be eliminated. The neutrino energy density is often not taken as an independent parameter. Provided the neutrino sector has the standard interactions, the neutrino energy density,

while relativistic, can be related to the photon density using thermal physics arguments, and it is currently difficult to see the effect of the neutrino mass, although observations of large-scale structure have already placed interesting upper limits. This reduces the standard parameter set to nine. In addition, there is no observational evidence for the existence of tensor perturbations (though the upper limits are quite weak), and so r could be set to zero. Presently n is in a somewhat controversial position regarding whether it needs to be varied in a fit, or can be set to the Harrison–Zel'dovich value $n = 1$. Parameter estimation [2] suggests $n = 1$ is ruled out at reasonable significance, but Bayesian model selection techniques [9] suggest the data is not conclusive. With n set to one, this leaves seven parameters, which is the smallest set that can usefully be compared to the present cosmological data set. This model (usually with n kept as a parameter) is referred to by various names, including ΛCDM, the concordance cosmology, and the standard cosmological model.

Of these parameters, only $\Omega_{\rm r}$ is accurately measured directly. The radiation density is dominated by the energy in the cosmic microwave background, and the COBE FIRAS experiment has determined its temperature to be $T = 2.725 \pm 0.001$ Kelvin [10], corresponding to $\Omega_{\rm r} = 2.47 \times 10^{-5} h^{-2}$. It typically does not need to be varied in fitting other data. If galaxy clustering data is not included in a fit, then the bias parameter is also unnecessary.

In addition to this minimal set, there is a range of other parameters which might prove important in future as the dataset further improves, but for which there is so far no direct evidence, allowing them to be set to a specific value. We discuss various speculative options in the next section. For completeness at this point, we mention one other interesting parameter, the helium fraction, which is a non-zero parameter that can affect the microwave anisotropies at a subtle level. Presently, big-bang nucleosynthesis provides the best measurement of this parameter, and it is usually fixed in microwave anisotropy studies, but the data are just reaching a level where allowing its variation may become mandatory.

21.1.5. *Derived parameters* :

The parameter list of the previous subsection is sufficient to give a complete description of cosmological models which agree with observational data. However, it is not a unique parametrization, and one could instead use parameters derived from that basic set. Parameters which can be obtained from the set given above include the age of the Universe, the present horizon distance, the present microwave background and neutrino background temperatures, the epoch of matter–radiation equality, the epochs of recombination and decoupling, the epoch of transition to an accelerating Universe, the baryon-to-photon ratio, and the baryon to dark matter density ratio. The physical densities of the matter components, $\Omega_i h^2$, are often more useful than the density parameters. The density perturbation amplitude can be specified in many different ways other than the large-scale primordial amplitude, for instance, in terms of its effect on the cosmic microwave background, or by specifying a short-scale quantity, a common choice being the present linear-theory mass dispersion on a scale of $8\,h^{-1}$Mpc, known as σ_8.

Different types of observation are sensitive to different subsets of the full cosmological parameter set, and some are more naturally interpreted in terms of some of the derived parameters of this subsection than on the original base parameter set. In particular, most types of observation feature degeneracies whereby they are unable to separate the effects of simultaneously varying several of the base parameters.

21.2. Extensions to the standard model

This section discusses some ways in which the standard model could be extended. At present, there is no positive evidence in favor of any of these possibilities, which are becoming increasingly constrained by the data, though there always remains the possibility of trace effects at a level below present observational capability.

21.2.1. *More general perturbations* :

The standard cosmology assumes adiabatic, Gaussian perturbations. Adiabaticity means that all types of material in the Universe share a common perturbation, so that if the space-time is foliated by constant-density hypersurfaces, then all fluids and fields are homogeneous on those slices, with the perturbations completely described by the variation of the spatial curvature of the slices. Gaussianity means that the initial perturbations obey Gaussian statistics, with the amplitudes of waves of different wavenumbers being randomly drawn from a Gaussian distribution of width given by the power spectrum. Note that gravitational instability generates non-Gaussianity; in this context, Gaussianity refers to a property of the initial perturbations before they evolve significantly.

The simplest inflation models, based on one dynamical field, predict adiabatic fluctuations and a level of non-Gaussianity which is too small to be detected by any experiment so far conceived. For present data, the primordial spectra are usually assumed to be power laws.

21.2.1.1. *Non-power-law spectra:*

For typical inflation models, it is an approximation to take the spectra as power laws, albeit usually a good one. As data quality improves, one might expect this approximation to come under pressure, requiring a more accurate description of the initial spectra, particularly for the density perturbations. In general, one can write a Taylor expansion of $\ln \Delta^2_{\mathcal{R}}$ as

$$\ln \Delta^2_{\mathcal{R}}(k) = \ln \Delta^2_{\mathcal{R}}(k_*) + (n_* - 1) \ln \frac{k}{k_*} + \frac{1}{2} \left. \frac{dn}{d \ln k} \right|_* \ln^2 \frac{k}{k_*} + \cdots , \qquad (21.9)$$

where the coefficients are all evaluated at some scale k_*. The term $dn/d\ln k|_*$ is often called the running of the spectral index [11]. Once non-power-law spectra are allowed, it is necessary to specify the scale k_* at which the spectral index is defined.

21.2.1.2. *Isocurvature perturbations:*

An isocurvature perturbation is one which leaves the total density unperturbed, while perturbing the relative amounts of different materials. If the Universe contains N fluids, there is one growing adiabatic mode and $N-1$ growing isocurvature modes. These can be excited, for example, in inflationary models where there are two or more fields which acquire dynamically-important perturbations. If one field decays to form normal matter, while the second survives to become the dark matter, this will generate a cold dark matter isocurvature perturbation.

In general, there are also correlations between the different modes, and so the full set of perturbations is described by a matrix giving the spectra and their correlations. Constraining such a general construct is challenging, though constraints on individual modes are beginning to become meaningful, with no evidence that any other than the adiabatic mode must be non-zero.

21.2.1.3. *Non-Gaussianity:*

Multi-field inflation models can also generate primordial non-Gaussianity. The extra fields can either be in the same sector of the underlying theory as the inflation, or completely separate, an interesting example of the latter being the curvaton model [12]. Current upper limits on non-Gaussianity are becoming stringent, but there remains much scope to push down those limits and perhaps reveal trace non-Gaussianity in the data. If non-Gaussianity is observed, its nature may favor an inflationary origin, or a different one such as topological defects. A plausible possibility is non-Gaussianity caused by defects forming in a phase transition which ended inflation.

21.2.2. ***Dark matter properties*** :

Dark matter properties are discussed in the article by Drees and Gerbier in this volume. The simplest assumption concerning the dark matter is that it has no significant interactions with other matter, and that its particles have a negligible velocity. Such dark matter is described as 'cold,' and candidates include the lightest supersymmetric particle, the axion, and primordial black holes. As far as astrophysicists are concerned, a complete specification of the relevant cold dark matter properties is given by the density parameter $\Omega_{\rm cdm}$, though those seeking to directly detect it are as interested in its interaction properties.

Cold dark matter is the standard assumption and gives an excellent fit to observations, except possibly on the shortest scales where there remains some controversy concerning the structure of dwarf galaxies and possible substructure in galaxy halos. For all the dark matter to have a large velocity dispersion, so-called hot dark matter,, has long been excluded, as it does not permit galaxies to form; for thermal relics the mass must be above about 1 keV to satisfy this constraint, though relics produced non-thermally, such as the axion, need not obey this limit. However, there remains the possibility that further parameters might need to be introduced to describe dark matter properties relevant to astrophysical observations. Suggestions which have been made include a modest velocity dispersion (warm dark matter) and dark matter self-interactions. There remains the possibility that the dark matter comprises two separate components, *e.g.*, a cold one and a hot one, an example being if massive neutrinos have a non-negligible effect.

21.2.3. ***Dark energy*** :

While the standard cosmological model given above features a cosmological constant, in order to explain observations indicating that the Universe is presently accelerating, further possibilities exist under the general heading dark energy.† A particularly attractive possibility (usually called quintessence, though that word is used with various different meanings in the literature) is that a scalar field is responsible, with the mechanism mimicking that of early Universe inflation [13]. As described by Olive and Peacock, a fairly model-independent description of dark energy can be given just using the equation of state parameter w, with $w = -1$ corresponding to a cosmological constant. In general, the function w could itself vary with redshift, though practical experiments devised so far would be sensitive primarily to some average value weighted over recent epochs. For high-precision predictions of microwave background anisotropies, it is better to use a scalar-field description in order to have a self-consistent evolution of the 'sound speed' associated with the dark energy perturbations.

A competing possibility is that the observed acceleration is due to a modification of gravity, *i.e.*, the left-hand side of Einstein's equation rather than the right. Observations of expansion kinematics alone cannot distinguish these two possibilities, but future probes of the growth rate of structure formation may be able to.

Present observations are consistent with a cosmological constant, but it is quite common to see w kept as a free parameter to be added to the set described in the previous section. Most, but not all, researchers assume the weak energy condition $w \geq -1$. In the future, it may be necessary to use a more sophisticated parametrization of the dark energy.

21.2.4. ***Complex ionization history*** :

The full ionization history of the Universe is given by specifying the ionization fraction as a function of redshift z. The simplest scenario takes the ionization to be zero from recombination up to some redshift $z_{\rm ion}$, at which point the Universe instantaneously re-ionizes completely. In that case, there is a one-to-one correspondence between τ and $z_{\rm ion}$ (that relation, however, also depending on other cosmological parameters).

While simple models of the re-ionization process suggest that rapid ionization is a good approximation, observational evidence is mixed, with indications of a high optical depth inferred from the microwave background difficult to reconcile with absorption seen in some high-redshift quasar systems, and also perhaps with the temperature of the intergalactic medium at $z \simeq 3$. Accordingly, a more complex ionization history may need to be considered, and perhaps separate histories for hydrogen and helium, which will necessitate new parameters. Additionally, high-precision microwave anisotropy experiments may require consideration of the level of residual ionization left after recombination, which in principle is computable from the other cosmological parameters.

† Unfortunately this is rather a misnomer, as it is the negative pressure of this material, rather than its energy, that is responsible for giving the acceleration. Furthermore, while generally in physics matter and energy are interchangeable terms, dark matter and dark energy are quite distinct concepts.

21.2.5. *Varying 'constants'* :

Variation of the fundamental constants of Nature over cosmological times is another possible enhancement of the standard cosmology. There is a long history of study of variation of the gravitational constant G, and more recently attention has been drawn to the possibility of small fractional variations in the fine-structure constant. There is presently no observational evidence for the former, which is tightly constrained by a variety of measurements. Evidence for the latter has been claimed from studies of spectral line shifts in quasar spectra at redshifts of order two [14], but this is presently controversial and in need of further observational study.

More broadly, one can ask whether general relativity is valid at all epochs under consideration.

21.2.6. *Cosmic topology* :

The usual hypothesis is that the Universe has the simplest topology consistent with its geometry, for example that a flat Universe extends forever. Observations cannot tell us whether that is true, but they can test the possibility of a non-trivial topology on scales up to roughly the present Hubble scale. Extra parameters would be needed to specify both the type and scale of the topology, for example, a cuboidal topology would need specification of the three principal axis lengths. At present, there is no direct evidence for cosmic topology, though the low values of the observed cosmic microwave quadrupole and octupole have been cited as a possible signature.

21.3. Probes

The goal of the observational cosmologist is to utilize astronomical objects to derive cosmological parameters. The transformation from the observables to the key parameters usually involves many assumptions about the nature of the objects, as well as about the nature of the dark matter. Below we outline the physical processes involved in each probe, and the main recent results. The first two subsections concern probes of the homogeneous Universe, while the remainder consider constraints from perturbations.

We note three types of uncertainties that enter into any errors on the cosmological parameters of interest: (i) due to the assumptions on the cosmological model and its priors (*i.e.*, the number of assumed cosmological parameters and their allowed range); (ii) due to the uncertainty in the astrophysics of the objects (*e.g.*, the mass–temperature relation of galaxy clusters); and (iii) due to instrumental and observational limitations (*e.g.*, the effect of 'seeing' on weak gravitational lensing measurements).

21.3.1. *Direct measures of the Hubble constant* :

In 1929, Edwin Hubble discovered the law of expansion of the Universe by measuring distances to nearby galaxies. The slope of the relation between the distance and recession velocity is defined to be the Hubble constant H_0. Astronomers argued for decades on the systematic uncertainties in various methods and derived values over the wide range, $40\,\mathrm{km\,s^{-1}\,Mpc^{-1}} \lesssim H_0 \lesssim 100\,\mathrm{km\,s^{-1}\,Mpc^{-1}}$.

One of the most reliable results on the Hubble constant comes from the Hubble Space Telescope Key Project [15]. The group has used the empirical period–luminosity

relations for Cepheid variable stars to obtain distances to 31 galaxies, and calibrated a number of secondary distance indicators (Type Ia Supernovae, Tully-Fisher, surface brightness fluctuations, and Type II Supernovae) measured over distances of 400 to 600 Mpc. They estimated $H_0 = 72 \pm 3$ (statistical) ± 7 (systematic) $\mathrm{km\,s^{-1}\,Mpc^{-1}}$.‡ The major sources of uncertainty in this result are due to the metallicity of the Cepheids and the distance to the fiducial nearby galaxy (called the Large Magellanic Cloud) relative to which all Cepheid distances are measured. Nevertheless, it is remarkable that this result is in such good agreement with the result derived from the WMAP CMB measurements (see Table 21.2).

21.3.2. *Supernovae as cosmological probes* :

The relation between observed flux and the intrinsic luminosity of an object depends on the luminosity distance d_L, which in turn depends on cosmological parameters. More specifically

$$d_L = (1+z) r_e(z)\,, \tag{21.10}$$

where $r_e(z)$ is the coordinate distance. For example, in a flat Universe

$$r_e(z) = \int_0^z dz'/H(z')\,. \tag{21.11}$$

For a general dark energy equation of state $w(z) = p_Q(z)/\rho_Q(z)$, the Hubble parameter is, still considering only the flat case,

$$H^2(z)/H_0^2 = (1+z)^3\Omega_{\rm m} + \Omega_Q \exp[3X(z)]\,, \tag{21.12}$$

where

$$X(z) = \int_0^z [1+w(z')](1+z')^{-1}dz'\,, \tag{21.13}$$

and $\Omega_{\rm m}$ and Ω_Q are the present density parameters of matter and dark energy components. If a general equation of state is allowed, then one has to solve for $w(z)$ (parametrized, for example, as $w(z) = w = \text{const.}$, or $w(z) = w_0 + w_1 z$) as well as for Ω_Q.

Empirically, the peak luminosity of supernova of Type Ia (SNe Ia) can be used as an efficient distance indicator (*e.g.*, Ref. 16). The favorite theoretical explanation for SNe Ia is the thermonuclear disruption of carbon-oxygen white dwarfs. Although not perfect 'standard candles,' it has been demonstrated that by correcting for a relation between the light curve shape and the luminosity at maximum brightness, the dispersion of the measured luminosities can be greatly reduced. There are several possible systematic effects which may affect the accuracy of the SNe Ia as distance indicators, for example, evolution with redshift and interstellar extinction in the host galaxy and in the Milky Way, but there is no indication that any of these effects are significant for the cosmological constraints.

‡ Unless stated otherwise, all quoted uncertainties in this article are one-sigma/68% confidence. It is common for cosmological parameters to have significantly non-Gaussian error distributions.

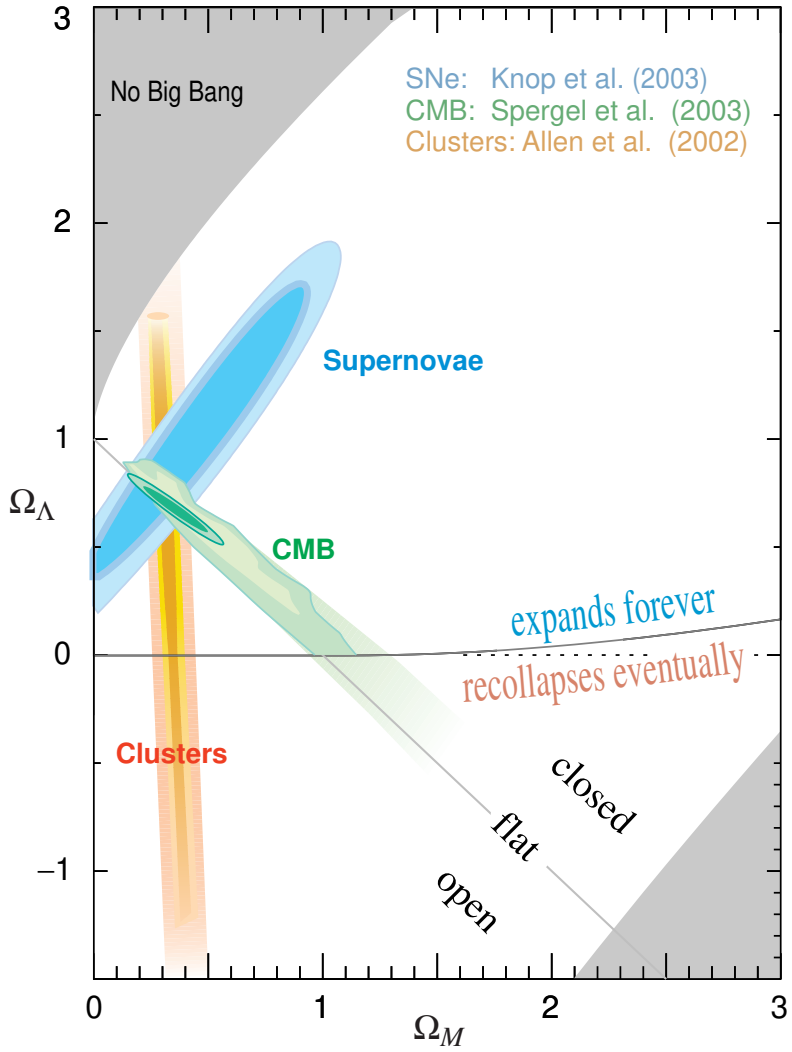

Figure 21.1: This shows the preferred region in the $\Omega_{\rm m}$–Ω_Λ plane from the compilation of supernovae data in Ref. 18, and also the complementary results coming from some other observations. See full-color version on color pages at end of book. [Courtesy of the Supernova Cosmology Project.]

Two major studies, the 'Supernova Cosmology Project' and the 'High-z Supernova Search Team," found evidence for an accelerating Universe [17], interpreted as due to a cosmological constant, or to a more general 'dark energy' component. Current results from the Supernova Cosmology Project [18] are shown in Fig. 21.1 (see also Ref. 19). The SNe Ia data alone can only constrain a combination of $\Omega_{\rm m}$ and Ω_Λ. When combined with the CMB data (which indicates flatness, *i.e.*, $\Omega_{\rm m} + \Omega_\Lambda \approx 1$), the best-fit values are $\Omega_{\rm m} \approx 0.3$ and $\Omega_\Lambda \approx 0.7$. Most results in the literature are consistent with Einstein's $w = -1$ cosmological constant case. For example, Wood-Vasey *et al.* [20] combined data from the ESSENCE and SNLS surveys and deduced $w = -1.07 \pm 0.09$ (stat 1σ) $\pm$ 0.13

(sys), $\Omega_{\rm m} = 0.267^{+0.028}_{-0.018}$ (stat 1σ).

Future experiments will aim to set constraints on the cosmic equation of state $w(z)$. However, given the integral relation between the luminosity distance and $w(z)$, it is not straightforward to recover $w(z)$ (*e.g.*, Ref. 21).

21.3.3. *Cosmic microwave background* :

The physics of the cosmic microwave background (CMB) is described in detail by Scott and Smoot in this volume. Before recombination, the baryons and photons are tightly coupled, and the perturbations oscillate in the potential wells generated primarily by the dark matter perturbations. After decoupling, the baryons are free to collapse into those potential wells. The CMB carries a record of conditions at the time of decoupling, often called primary anisotropies. In addition, it is affected by various processes as it propagates towards us, including the effect of a time-varying gravitational potential (the integrated Sachs-Wolfe effect), gravitational lensing, and scattering from ionized gas at low redshift.

The primary anisotropies, the integrated Sachs-Wolfe effect, and scattering from a homogeneous distribution of ionized gas, can all be calculated using linear perturbation theory, a widely-used implementation being the CMBFAST code of Seljak and Zaldarriaga [6] (CAMB is a popular alternative, often used embedded in the analyis package CosmoMC [7]) . Gravitational lensing is also calculated in this code. Secondary effects such as inhomogeneities in the re-ionization process, and scattering from gravitationally-collapsed gas (the Sunyaev–Zel'dovich effect), require more complicated, and more uncertain, calculations.

The upshot is that the detailed pattern of anisotropies, quantified, for instance, by the angular power spectrum C_ℓ, depends on all of the cosmological parameters. In a typical cosmology, the anisotropy power spectrum [usually plotted as $\ell(\ell+1)C_\ell$] features a flat plateau at large angular scales (small ℓ), followed by a series of oscillatory features at higher angular scales, the first and most prominent being at around one degree ($\ell \simeq 200$). These features, known as acoustic peaks, represent the oscillations of the photon-baryon fluid around the time of decoupling. Some features can be closely related to specific parameters—for instance, the location of the first peak probes the spatial geometry, while the relative heights of the peaks probes the baryon density—but many other parameters combine to determine the overall shape.

The three-year data release from the WMAP satellite [1], henceforth WMAP3, has provided the most accurate results to date on the spectrum of CMB fluctuations, with a precision determination of the temperature power spectrum up to $\ell \simeq 900$, shown in Fig. 21.2, and the best measurements of the spectrum of E-polarization anisotropies and the correlation spectrum between temperature and polarization (those spectra having first been detected by DASI [22]) . These are consistent with models based on the parameters we have described, and provide quite accurate determinations of many of them [2]. In this subsection, we will refer to results from WMAP alone, with the following section studying some combinations with other observations. We note that as the parameter fitting is done in a multi-parameter space, one has to assume a 'prior' range for each of the parameters (*e.g.*, Hubble constant $0.5 < h < 1$), and there may be some dependence

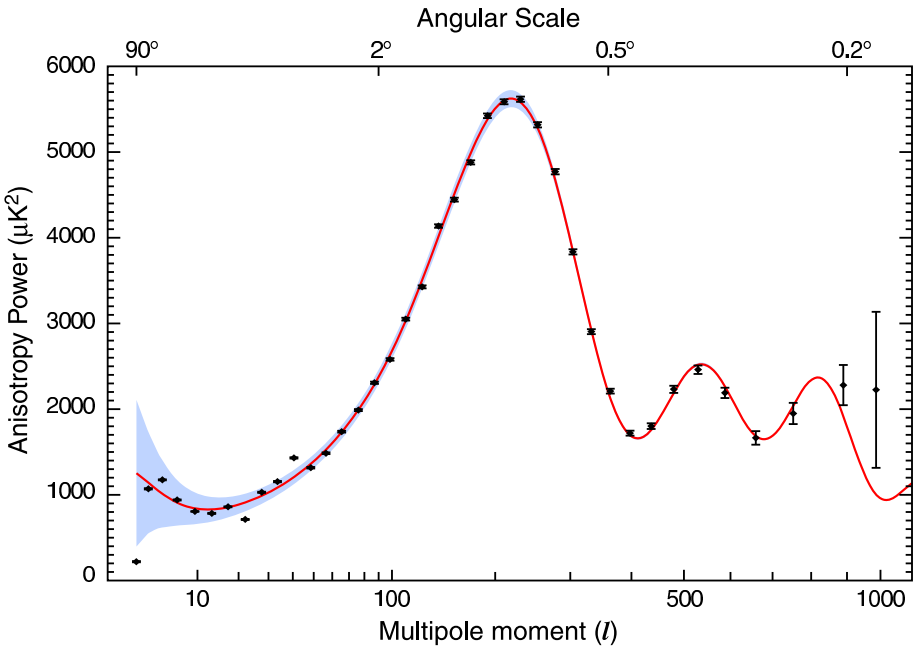

Figure 21.2: The angular power spectrum of the cosmic microwave background temperature from WMAP3. The solid line shows the prediction from the best-fitting ΛCDM model [2]. The error bars on the data points (which are tiny for most of them) indicate the observational errors, while the shaded region indicates the statistical uncertainty from being able to observe only one microwave sky, known as cosmic variance, which is the dominant uncertainty on large angular scales. See full-color version on color pages at end of book. [Figure courtesy NASA/WMAP Science Team.]

on these assumed priors.

WMAP3 provides an exquisite measurement of the location of the first acoustic peak, which directly probes the spatial geometry and yields a total density $\Omega_{\rm tot} \equiv \sum \Omega_i + \Omega_\Lambda$ of

$$\Omega_{\rm tot} = 1.011 \pm 0.012\,, \tag{21.14}$$

consistent with spatial flatness and completely excluding significantly curved Universes. (This result does however require constraints on the Hubble parameter from other measurements, in this case the SNLS supernovae; WMAP3 alone constrains $\Omega_{\rm tot}$ only weakly, and allows significantly closed Universes if h is small. This result also assumes that the dark energy is a cosmological constant.) WMAP3 also gives a precision measurement of the age of the Universe. It gives a baryon density consistent with, and at much higher precision than, that coming from nucleosynthesis. It affirms the need for both dark matter and dark energy if the data are to be explained. It shows no evidence for dynamics of the dark energy, being consistent with a pure cosmological constant ($w = -1$).

The density perturbations are consistent with a power-law primordial spectrum. There are indications that the spectral slope is less than the Harrison–Zel'dovich value

$n = 1$ [2], though the result appears less strong using Bayesian techniques [9]. There is no indication of tensor perturbations, but the upper limit is quite weak.

WMAP3 gives a much lower result for the reionization optical depth τ than did their first year results [23]. The current best-fit value $\tau = 0.089$ is in reasonable agreement with models of how early structure formation induces reionization.

WMAP3 is consistent with other experiments and its dynamic range can be enhanced by including information from small-angle CMB experiments including ACBAR, CBI and VSA. However the WMAP3 dataset on its own is so powerful that these add little constraining power.

21.3.4. *Galaxy clustering* :

The power spectrum of density perturbations depends on the nature of the dark matter. Within the Cold Dark Matter model, the shape of the power spectrum depends primarily on the primordial power spectrum and on the combination $\Omega_{\rm m}h$ which determines the horizon scale at matter–radiation equality, with a subdominant dependence on the baryon density. The matter distribution is most easily probed by observing the galaxy distribution, but this must be done with care as the galaxies do not perfectly trace the dark matter distribution. Rather, they are a 'biased' tracer of the dark matter. The need to allow for such bias is emphasized by the observation that different types of galaxies show bias with respect to each other. Further, the observed 3D galaxy distribution is in redshift space, *i.e.*, the observed redshift is the sum of the Hubble expansion and the line-of-sight peculiar velocity, leading to linear and non-linear dynamical effects which also depend on the cosmological parameters. On the largest length scales, the galaxies are expected to trace the location of the dark matter, except for a constant multiplier b to the power spectrum, known as the linear bias parameter. On scales smaller than 20 h^{-1} Mpc or so, the clustering pattern is 'squashed' in the radial direction due to coherent infall, which depends on the parameter $\beta \equiv \Omega_{\rm m}^{0.6}/b$ (on these shorter scales, more complicated forms of biasing are not excluded by the data). On scales of a few h^{-1} Mpc, there is an effect of elongation along the line of sight (colloquially known as the 'finger of God' effect) which depends on the galaxy velocity dispersion $\sigma_{\rm p}$.

21.3.4.1. *The galaxy power spectrum:*

The 2-degree Field (2dF) Galaxy Redshift Survey is now complete and publicly available.** The power-spectrum analysis of the final 2dFGRS data set of approximately 220,000 galaxies was fitted to a CDM model [24]. It shows evidence for baryon acoustic oscillations, with baryon fraction $\Omega_{\rm b}/\Omega_{\rm m} = 0.185 \pm 0.046$ (1-σ uncertainties). The shape of the power spectrum is characterized by $\Omega_{\rm m}h = 0.168 \pm 0.016$, and in combination with WMAP data gives $\Omega_{\rm m} = 0.231 \pm 0.021$ (see also Ref. 25). The 2dF power spectrum is compared with the Sloan Digital Sky Survey (SDSS) †† power spectrum [26] in Fig. 21.3. We see agreement in the gross features, but also some discrepancies. Eisenstein *et al.* [27] reported on detection of baryon acoustic peak in the large-scale correlation function

** See `http://www.mso.anu.edu.au/2dFGRS`

†† See `http://www.sdss.org`

of the SDSS sample of nearly 47,000 Luminous Red Galaxies (LRG). By using the baryon acoustic peak as a 'standard ruler' they found, independent of WMAP, that $\Omega_{\rm m} = 0.273 \pm 0.025$ for a flat ΛCDM model. A combination of the 2dF, the SDSS main and the LRG samples [28] yield from the baryon oscillation signals $\Omega_{\rm m} = 0.249 \pm 0.018$ and $w = -1.004 \pm 0.089$, assuming a flat universe and constraints from SN Ia and CMB data. Signatures of baryon acoustic oscillations have also been measured [29,30] from samples nearly 600,000 LRGs with photometric redshifts (which are less accurate than spectroscopic redshifts, but easier to obtain for large samples).

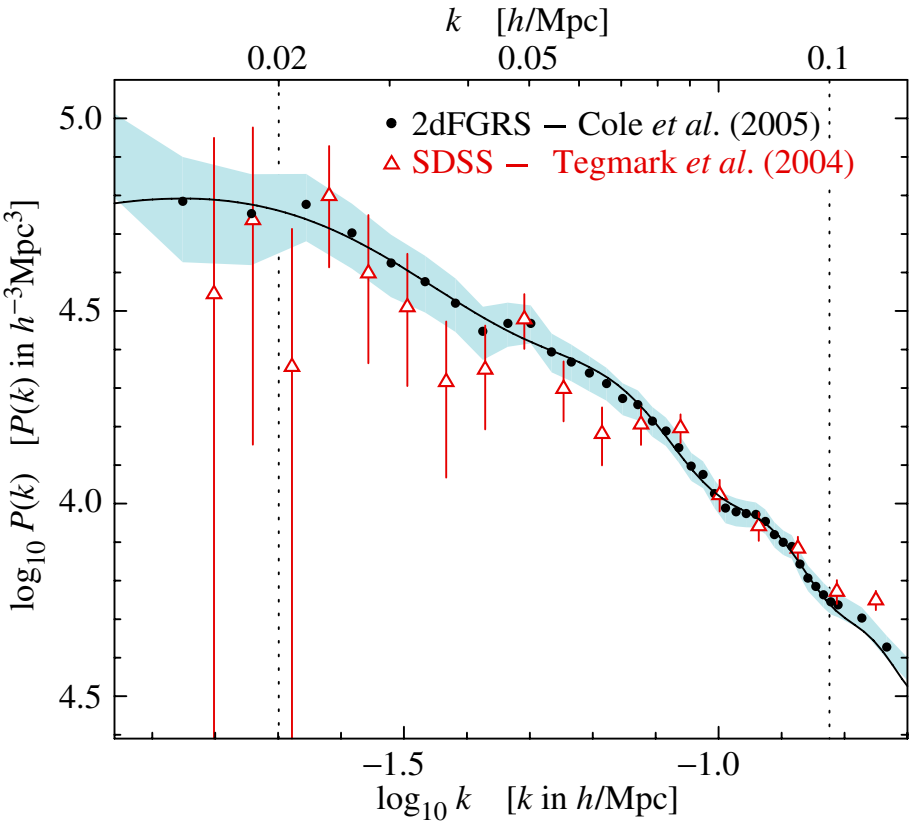

Figure 21.3: The galaxy power spectrum from the 2dF galaxy redshift survey [24] compared with that from SDSS [26], each corrected for its survey geometry. The 2dFGRS power spectrum (with distances measured in redshift space) is shown by solid circles with one-sigma errors shown by the shaded area. The triangles and error bars show the SDSS power spectrum. The solid curve shows a linear-theory ΛCDM model with $\Omega_{\rm m}h = 0.168$, $\Omega_{\rm b}/\Omega_{\rm m} = 0.17$, $h = 0.72$, $n = 1$ and normalization matched to the 2dFGRS power spectrum. The dotted vertical lines indicate the range over which the best-fit model was evaluated. See full-color version on color pages at end of book. [Figure provided by Shaun Cole and Will Percival; see Ref. 24.]

Combination of the 2dF data with the CMB indicates a 'biasing' parameter $b \sim 1$, in agreement with a 2dF-alone analysis of higher-order clustering statistics. However, results for biasing also depend on the length scale over which a fit is done, and the selection of

the objects by luminosity, spectral type, or color. In particular, on scales smaller than 10 h^{-1}Mpc, different galaxy types are clustered differently. This 'biasing' introduces a systematic effect on the determination of cosmological parameters from redshift surveys. Prior knowledge from simulations of galaxy formation could help, but is model-dependent. We also note that the present-epoch power spectrum is not sensitive to dark energy, so it is mainly a probe of the matter density.

21.3.4.2. *Limits on neutrino mass from galaxy surveys and other probes:*

Large-scale structure data can put an upper limit on the ratio $\Omega_\nu/\Omega_{\rm m}$ due to the neutrino 'free streaming' effect [31,32]. For example, by comparing the 2dF galaxy power spectrum with a four-component model (baryons, cold dark matter, a cosmological constant, and massive neutrinos), it was estimated that $\Omega_\nu/\Omega_{\rm m} < 0.13$ (95% confidence limit), giving $\Omega_\nu < 0.04$ if a concordance prior of $\Omega_{\rm m} = 0.3$ is imposed. The latter corresponds to an upper limit of about 2 eV on the total neutrino mass, assuming a prior of $h \approx 0.7$ [33]. Potential systematic effects include biasing of the galaxy distribution and non-linearities of the power spectrum. A similar upper limit of 2 eV was derived from CMB anisotropies alone [2,34,35]. The above analyses assume that the primordial power spectrum is adiabatic, scale-invariant and Gaussian. Additional cosmological data sets bring down this upper limit [36,37]. An upper limit on the total neutrino mass of 0.17 eV was reported by combining a large number of cosmological probes [38].

Laboratory limits on absolute neutrino masses from tritium beta decay and especially from neutrinoless double-beta decay should, within the next decade, push down towards (or perhaps even beyond) the 0.1 eV level that has cosmological significance.

21.3.5. ***Clusters of galaxies*** :

A cluster of galaxies is a large collection of galaxies held together by their mutual gravitational attraction. The largest ones are around 10^{15} solar masses, and are the largest gravitationally-collapsed structures in the Universe. Even at the present epoch they are relatively rare, with only a few percent of galaxies being in clusters. They provide various ways to study the cosmological parameters; here we discuss constraints from the measurements of the cluster number density and the baryon fraction in clusters.

21.3.5.1. *Cluster number density:*

The first objects of a given kind form at the rare high peaks of the density distribution, and if the primordial density perturbations are Gaussian-distributed, their number density is exponentially sensitive to the size of the perturbations, and hence can strongly constrain it. Clusters are an ideal application in the present Universe. They are usually used to constrain the amplitude σ_8, as a box of side $8\,h^{-1}$ Mpc contains about the right amount of material to form a cluster. The most useful observations at present are of X-ray emission from hot gas lying within the cluster, whose temperature is typically a few keV, and which can be used to estimate the mass of the cluster. A theoretical prediction for the mass function of clusters can come either from semi-analytic arguments or from numerical simulations. At present, the main uncertainty is the relation between the observed gas temperature and the cluster mass, despite extensive study using simulations.

Ref. [39] gives

$$\sigma_8 = 0.78^{+0.30}_{-0.06} \qquad (95\% \text{ confidence}) \tag{21.15}$$

for $\Omega_{\rm m} = 0.35$, with highly non-Gaussian error bars, but different authors still find a spread of values. Scaling to lower $\Omega_{\rm m}$ increases σ_8. This result is somewhat above the values predicted in cosmologies compatible with WMAP3.

The same approach can be adopted at high redshift (which for clusters means redshifts approaching one) to attempt to measure σ_8 at an earlier epoch. The evolution of σ_8 is primarily driven by the value of the matter density $\Omega_{\rm m}$, with a sub-dominant dependence on the dark energy density. It is generally recognized that such analyses favor a low matter density, though there is not complete consensus on this, and at present this technique for constraining the density is not competitive with the CMB.

21.3.5.2. *Cluster baryon fraction:*

If clusters are representative of the mass distribution in the Universe, the fraction of the mass in baryons to the overall mass distribution would be $f_{\rm b} = \Omega_{\rm b}/\Omega_{\rm m}$. If $\Omega_{\rm b}$, the baryon density parameter, can be inferred from the primordial nucleosynthesis abundance of the light elements, the cluster baryon fraction $f_{\rm b}$ can then be used to constrain $\Omega_{\rm m}$ and h (*e.g.*, Ref. 40). The baryons in clusters are primarily in the form of X-ray-emitting gas that falls into the cluster, and secondarily in the form of stellar baryonic mass. Hence, the baryon fraction in clusters is estimated to be

$$f_{\rm b} = \frac{\Omega_{\rm b}}{\Omega_{\rm m}} \simeq f_{\rm gas} + f_{\rm gal}\,, \tag{21.16}$$

where $f_{\rm b} = M_{\rm b}/M_{\rm grav}$, $f_{\rm gas} = M_{\rm gas}/M_{\rm grav}$, $f_{\rm gal} = M_{\rm gal}/M_{\rm grav}$, and $M_{\rm grav}$ is the total gravitating mass.

This can be used to obtain an approximate relation between $\Omega_{\rm m}$ and h:

$$\Omega_{\rm m} = \frac{\Omega_{\rm b}}{f_{\rm gas} + f_{\rm gal}} \simeq \frac{\Omega_{\rm b}}{0.08h^{-1.5} + 0.01h^{-1}}\,. \tag{21.17}$$

Big Bang Nucleosynthesis gives $\Omega_{\rm b}h^2 \approx 0.02$, allowing the above relation to be approximated as $\Omega_{\rm m}h^{0.5} \approx 0.25$ (*e.g.*, Ref. 41). For example, Allen *et al.* [42] derived a density parameter consistent with $\Omega_{\rm m} = 0.3$ from Chandra observations.

21.3.6. ***Clustering in the inter-galactic medium*** :

It is commonly assumed, based on hydrodynamic simulations, that the neutral hydrogen in the inter-galactic medium (IGM) can be related to the underlying mass distribution. It is then possible to estimate the matter power spectrum on scales of a few megaparsecs from the absorption observed in quasar spectra, the so-called Lyman-alpha forest. The usual procedure is to measure the power spectrum of the transmitted flux, and then to infer the mass power spectrum. Photo-ionization heating by the ultraviolet background radiation and adiabatic cooling by the expansion of the Universe combine to give a simple power-law relation between the gas temperature and the baryon density.

It also follows that there is a power-law relation between the optical depth τ and $\rho_{\rm b}$. Therefore, the observed flux $F = \exp(-\tau)$ is strongly correlated with $\rho_{\rm b}$, which itself traces the mass density. The matter and flux power spectra can be related by

$$P_{\rm m}(k) = b^2(k)\, P_F(k)\,, \tag{21.18}$$

where $b(k)$ is a bias function which is calibrated from simulations. Croft *et al.* [43] derived cosmological parameters from Keck Telescope observations of the Lyman-alpha forest at redshifts $z = 2 - 4$. Their derived power spectrum corresponds to that of a CDM model, which is in good agreement with the 2dF galaxy power spectrum. A recent study using VLT spectra [44] agrees with the flux power spectrum of Ref. 43. This method depends on various assumptions. Seljak *et al.* [45] pointed out that errors are sensitive to the range of cosmological parameters explored in the simulations, and the treatment of the mean transmitted flux.

21.3.7. *Gravitational lensing* :

Images of background galaxies get distorted due to the gravitational effect of mass fluctuations along the line of sight. Deep gravitational potential wells such as galaxy clusters generate 'strong lensing,' *i.e.*, arcs and arclets, while more moderate fluctuations give rise to 'weak lensing'. Weak lensing is now widely used to measure the mass power spectrum in random regions of the sky (see Ref. 46 for recent reviews). As the signal is weak, the CCD frame of deformed galaxy shapes ('shear map') is analyzed statistically to measure the power spectrum, higher moments, and cosmological parameters.

The shear measurements are mainly sensitive to the combination of $\Omega_{\rm m}$ and the amplitude σ_8. For example, the weak lensing signal detected by the CFHT Legacy Survey [47] translates into $\sigma_8 = 0.85 \pm 0.06$ for a fiducial $\Omega_{\rm m} = 0.3$ assuming a ΛCDM model. Earlier results are summarized in Ref. 46. There are various systematic effects in the interpretation of weak lensing, *e.g.*, due to atmospheric distortions during observations, the redshift distribution of the background galaxies, intrinsic correlation of galaxy shapes, and non-linear modeling uncertainties.

21.3.8. *Peculiar velocities* :

Deviations from the Hubble flow directly probe the mass fluctuations in the Universe, and hence provide a powerful probe of the dark matter. Peculiar velocities are deduced from the difference between the redshift and the distance of a galaxy. The observational difficulty is in accurately measuring distances to galaxies. Even the best distance indicators (*e.g.*, the Tully–Fisher relation) give an error of 15% per galaxy, hence limiting the application of the method at large distances. Peculiar velocities are mainly sensitive to $\Omega_{\rm m}$, not to Ω_Λ or quintessence. Extensive analyses in the early 1990s (*e.g.*, Ref. 48) suggested a value of $\Omega_{\rm m}$ close to unity. A more recent analysis [49], which takes into account non-linear corrections, gives $\sigma_8\Omega_{\rm m}^{0.6} = 0.49 \pm 0.06$ and $\sigma_8\Omega_{\rm m}^{0.6} = 0.63 \pm 0.08$ (90% errors) for two independent data sets. While at present cosmological parameters derived from peculiar velocities are strongly affected by random and systematic errors, a new generation of surveys may improve their accuracy. Three promising approaches are the 6dF near-infrared survey of 15,000 peculiar velocities[‡‡], supernovae Type Ia, and the

[‡‡] See `http://www.mso.anu.edu.au/6dFGS/`

kinematic Sunyaev–Zel'dovich effect.

21.4. Bringing observations together

Although it contains two ingredients—dark matter and dark energy—which have not yet been verified by laboratory experiments, the ΛCDM model is almost universally accepted by cosmologists as the best description of present data. The basic ingredients are given by the parameters listed in Sec. 21.1.4, with approximate values of some of the key parameters being $\Omega_{\rm b} \approx 0.04$, $\Omega_{\rm dm} \approx 0.20$, $\Omega_\Lambda \approx 0.76$, and a Hubble constant $h \approx 0.73$. The spatial geometry is very close to flat (and often assumed to be precisely flat), and the initial perturbations Gaussian, adiabatic, and nearly scale-invariant.

Table 21.2: Parameter constraints reproduced from Spergel *et al.* [2], with some additional rounding. All columns assume the ΛCDM cosmology with a power-law initial spectrum, no tensors, spatial flatness, and a cosmological constant as dark energy. Three different data combinations are shown to highlight the extent to which this choice matters. The first column is WMAP3 alone, the second combines this with 2dF, and the third column shows a combination of all datasets considered in Ref. 2. The perturbation amplitude is specified via the derived parameter σ_8; see Ref. 2 for details. Uncertainties are shown at one sigma, and caution is needed in extrapolating them to higher significance levels due to non-Gaussian likelihoods and assumed priors.

	WMAP alone	WMAP + 2dF	WMAP + all
$\Omega_{\rm m}h^2$	0.128 ± 0.008	0.126 ± 0.005	0.132 ± 0.004
$\Omega_{\rm b}h^2$	0.0223 ± 0.0007	0.0222 ± 0.0007	0.0219 ± 0.0007
h	0.73 ± 0.03	0.73 ± 0.02	$0.704^{+0.015}_{-0.016}$
n	0.958 ± 0.016	0.948 ± 0.015	0.947 ± 0.015
τ	0.089 ± 0.030	0.083 ± 0.028	$0.073^{+0.027}_{-0.028}$
σ_8	0.76 ± 0.05	0.74 ± 0.04	0.78 ± 0.03

The most powerful single experiment is WMAP3, which on its own supports all these main tenets. Values for some parameters, as given in Spergel *et al.* [2], are reproduced in Table 21.2. This model presumes a flat Universe, and so Ω_Λ is a derived quantity in this analysis, with best-fit value $\Omega_\Lambda = 0.76$.

These constraints can be somewhat strengthened by adding additional datasets, as shown in the Table. However, WMAP3 on its own is sufficiently powerful that inclusion

of other datasets only changes things at quite a detailed level. In our view, the most robust present constraints are those from WMAP3 alone.

The baryon density Ω_b is now measured with quite high accuracy from the CMB and large-scale structure, and is consistent with the determination from big bang nucleosynthesis; Fields and Sarkar in this volume quote the range $0.017 \leq \Omega_{\rm b} h^2 \leq 0.024$.

While Ω_Λ is measured to be non-zero with very high confidence, there is no evidence of evolution of the dark energy density. The WMAP team find the limit $w < -0.82$ at 95% confidence from a compilation of data including SNe Ia data, with the cosmological constant case $w = -1$ giving an excellent fit to the data.

The data provides strong support for the main predictions of the simplest inflation models: spatial flatness and adiabatic, Gaussian, nearly scale-invariant density perturbations. But it is disappointing that there is no sign of primordial gravitational waves, with WMAP3 providing only a weak upper limit $r < 0.65$ at 95% confidence [2] (this assumes no running, and weakens yet further if running is allowed). The spectral index n is placed in an interesting position by WMAP3, with indications that $n < 1$ is required by the data. However, the conclusion that $n = 1$ is ruled out that is suggested by parameter estimation [2] receives much less compelling support in Bayesian model selection analyses [9], and in our view, it is premature to conclude that $n = 1$ is no longer viable.

Tests have been made for various types of non-Gaussianity, a particular example being a parameter $f_{\rm NL}$ which measures a quadratic contribution to the perturbations and is constrained to $-54 < f_{\rm NL} < 114$ at 95% confidence [2] (this looks weak, but prominent non-Gaussianity requires the product $f_{\rm NL}\Delta_{\mathcal{R}}$ to be large, and $\Delta_{\mathcal{R}}$ is of order 10^{-5}).

Two parameters which are still uncertain are $\Omega_{\rm m}$ and σ_8, both of which were revised downwards significantly by WMAP3 to a level where they do not sit well against local measures of σ_8, particularly those using weak gravitational lensing. However an analysis including Lyman-alpha data with WMAP3 has found that this brings σ_8 up again [38]. It is clear that we have yet to reach the last word on these parameters. It is also worth noting that WMAP3 only probes larger length scales, and the constraint comes from using WMAP to estimate all the parameters of the model needed to determine σ_8. As such, their constraint depends strongly on the assumed set of cosmological parameters being sufficient.

One parameter which is surprisingly robust is the age of the Universe. There is a useful coincidence that for a flat Universe the position of the first peak is strongly correlated with the age of the Universe. The WMAP3 result is 13.7 ± 0.2 Gyr (assuming a flat Universe). This is in good agreement with the ages of the oldest globular clusters [50] and radioactive dating [51].

21.5. Outlook for the future

The concordance model is now well established, and there seems little room left for any dramatic revision of this paradigm. A measure of the strength of that statement is how difficult it has proven to formulate convincing alternatives. For example, one corner of parameter space that has been explored is the possibility of abandoning the dark energy, and instead considering a mixed dark matter model with $\Omega_{\rm m} = 1$ and $\Omega_\nu = 0.2$. Such a model fits both the 2dF and WMAP data reasonably well, but only for a Hubble constant $h < 0.5$ [33,52]. However, this model is inconsistent with the HST key project value of h, the results from SNe Ia, cluster number density evolution, and baryon fraction in clusters.

Should there indeed be no major revision of the current paradigm, we can expect future developments to take one of two directions. Either the existing parameter set will continue to prove sufficient to explain the data, with the parameters subject to ever-tightening constraints, or it will become necessary to deploy new parameters. The latter outcome would be very much the more interesting, offering a route towards understanding new physical processes relevant to the cosmological evolution. There are many possibilities on offer for striking discoveries, for example:

- The cosmological effects of a neutrino mass may be unambiguously detected, shedding light on fundamental neutrino properties;
- Compelling detection of deviations from scale-invariance in the initial perturbations would indicate dynamical processes during perturbation generation by, for instance, inflation;
- Detection of primordial non-Gaussianities would indicate that non-linear processes influence the perturbation generation mechanism;
- Detection of variation in the dark energy density (*i.e.*, $w \neq -1$) would provide much-needed experimental input into the question of the properties of the dark energy.

These provide more than enough motivation for continued efforts to test the cosmological model and improve its precision.

Over the coming years, there are a wide range of new observations, which will bring further precision to cosmological studies. Indeed, there are far too many for us to be able to mention them all here, and so we will just highlight a few areas.

The cosmic microwave background observations will improve in several directions. The new frontier is the study of polarization, first detected in 2002 by DASI and for which power spectrum measurements have now been made by WMAP and Boomerang [53]. Dedicated ground-based polarization experiments, such as CBI, QUaD, and Clover promise powerful measures of the polarization spectrum in the next few years, and may be able to separately detect the two modes of polarization. Another area of development is pushing accurate power spectrum measurements to smaller angular scales, typically achieved by interferometry, which should allow measurements of secondary anisotropy effects, such as the Sunyaev–Zel'dovich effect, whose detection has already been tentatively claimed by CBI. Finally, we mention the Planck satellite, due to launch in 2008, which will make high-precision all-sky maps of temperature and polarization, utilizing a very wide

frequency range for observations to improve understanding of foreground contaminants, and to compile a large sample of clusters via the Sunyaev–Zel'dovich effect.

On the supernova side, the most ambitious initiative at present is a proposed satellite mission JDEM (Joint Dark Energy Mission) funded by NASA and DOE. There are several candidates for this mission, including the much-publicized SNAP satellite, but the funding has yet to be secured. An impressive array of ground-based dark energy surveys are also already operational or proposed, including the ESSENCE project, the Dark Energy Survey, LSST, and WFMOS. With large samples, it may be possible to detect evolution of the dark energy density, thus measuring its equation of state and perhaps even its variation.

An exciting new area for the future will be radio surveys of the redshifted 21-cm line of hydrogen. Because of the intrinsic narrowness of this line, by tuning of the bandpass the emission from narrow redshift slices of the Universe will be measured to extremely high redshift, probing the details of the reionization process at redshifts up to perhaps 20. LOFAR is the first instrument able to do this and is at an advanced construction stage. In the medium term, the Square Kilometer Array (SKA) will take these studies to a precision level.

The above future surveys will address fundamental questions of physics well beyond just testing the 'concordance' ΛCDM model and minor variations. It would be important to distinguish the imprint of dark energy and dark matter on the geometry from the growth of perturbations, and to test theories of modified gravity as alternatives for fitting the observations to a Dark Energy component.

The development of the first precision cosmological model is a major achievement. However, it is important not to lose sight of the motivation for developing such a model, which is to understand the underlying physical processes at work governing the Universe's evolution. On that side, progress has been much less dramatic. For instance, there are many proposals for the nature of the dark matter, but no consensus as to which is correct. The nature of the dark energy remains a mystery. Even the baryon density, now measured to an accuracy of a few percent, lacks an underlying theory able to predict it even within orders of magnitude. Precision cosmology may have arrived, but at present many key questions remain unanswered.

Acknowledgements:

Both authors acknowledge PPARC Senior Research Fellowships. We thank Sarah Bridle and Jochen Weller for useful comments on this article, and OL thanks members of the Cambridge Leverhulme Quantitative Cosmology and 2dFGRS Teams for helpful discussions.

References:

1. G. Hinshaw *et al.*, Astrophys. J. Supp. **170**, 288 (2007);
   L. Page *et al.*, Astrophys. J. Supp. **170**, 335 (2007);
   N. Jarosik *et al.*, Astrophys. J. Supp. **170**, 263 (2007).
2. D. N. Spergel *et al.*, Astrophys. J. Supp **170**, 377 (2007).
3. S. Fukuda *et al.*, Phys. Rev. Lett. **85**, 3999 (2000);
   Q.R. Ahmad *et al.*, Phys. Rev. Lett. **87**, 071301 (2001).

4. A.D. Dolgov *et al.*, Nucl. Phys. **B632**, 363 (2002).
5. For detailed accounts of inflation see E.W. Kolb and M.S. Turner, *The Early Universe*, Addison–Wesley (Redwood City, 1990);
   A.R. Liddle and D.H. Lyth, *Cosmological Inflation and Large-Scale Structure*, (Cambridge University Press, 2000).
6. U. Seljak and M. Zaldarriaga, Astrophys. J. **469**, 1 (1996).
7. A. Lewis and S. Bridle, Phys. Rev. D**66**, 103511 (2002).
8. H.V. Peiris *et al.*, Astrophys. J. Supp. **148**, 213 (2003).
9. D. Parkinson *et al.*, Phys. Rev. D**73**, 123523 (2006).
10. J.C. Mather *et al.*, Astrophys. J. **512**, 511 (1999).
11. A. Kosowsky and M.S. Turner, Phys. Rev. **D52**, 1739 (1995).
12. D.H. Lyth and D. Wands, Phys. Lett. **B524**, 5 (2002);
    K. Enqvist and M.S. Sloth, Nucl. Phys. **B626**, 395 (2002);
    T. Moroi and T. Takahashi, Phys. Lett. **B522**, 215 (2001).
13. B. Ratra and P.J.E. Peebles, Phys. Rev. **D37**, 3406 (1988);
    C. Wetterich, Nucl. Phys. **B302**, 668 (1988);
    T. Padmanabhan, Phys. Rept. **380**, 235 (2003);
    V. Sahni and A. Starobinsky, Int. J. Mod. Phys. **D9**, 373 (2000).
14. J.K. Webb *et al.*, Phys. Rev. Lett. **82**, 884 (1999);
    J.K. Webb *et al.*, Phys. Rev. Lett. **87**, 091301 (2001);
    J.K. Webb *et al.*, Astrophys. Sp. Sci. **283**, 565 (2003);
    H. Chand *et al.*, Astron. Astrophys. **417**, 853 (2004);
    R. Srianand *et al.*, Phys. Rev. Lett. **92**, 121302 (2004).
15. W.L. Freedman *et al.*, Astrophys. J. **553**, 47 (2001).
16. A. Filippenko, `astro-ph/0307139`.
17. A.G. Riess *et al.*, Astron. J. **116**, 1009 (1998);
    P. Garnavich *et al.*, Astrophys. J. **509**, 74 (1998);
    S. Perlmutter *et al.*, Astrophys. J. **517**, 565 (1999).
18. R.A. Knop *et al.*, Astrophys. J. **598**, 102 (2003).
19. J.L. Tonry *et al.*, Astrophys. J. **594**, 1 (2003);
    A.G. Riess *et al.*, Astrophys. J. **659**, 98 (2007);
    S. Jha, A.G. Riess, and R.P. Kirshner *et al.*, Astrophys. J. **659**, 122 (2007).
20. Wood-Vasey, W.M. et al., `astro-ph/0701041`.
21. I. Maor *et al.*, Phys. Rev. **D65**, 123003 (2002).
22. J. Kovac *et al.*, Nature **420**, 772 (2002).
23. D.N. Spergel *et al.*, Astrophys. J. Supp. **148**, 175 (2003).
24. S. Cole *et al.*, Mon. Not. Roy. Astr. Soc. **362**, 505 (2005).
25. A. Sanchez *et al.*, Mon. Not. Roy. Astr. Soc. **366**, 189 (2006).
26. M. Tegmark *et al.*, Astrophys. J. **606**, 702 (2004).
27. D. Eisenstein *et al.*, Astrophys. J. **633**, 560 (2005).
28. W.J. Percival *et al.*, `arXiv:0705.3323` [astro-ph] (2007).
29. C. Blake *et al.*, Mon. Not. Roy. Astr. Soc. **374**, 1527 (2007).
30. N. Padmanabhan *et al.*, Mon. Not. Roy. Astr. Soc. **378**, 852 (2007).
31. W. Hu *et al.*, Phys. Rev. Lett. **80**, 5255 (1998).

32. J. Lesgourgues and S. Pastor, Physics Reports, **429**, 307 (2006).
33. O. Elgaroy and O. Lahav, JCAP **0304**, 004 (2003).
34. K. Ichikawa *et al.*, Phys. Rev. D**71**, 043001 (2005).
35. M. Fukugita *et al.*, Phys Rev D, **74**, 027302 (2006).
36. S. Hannestad, JCAP **0305**, 004 (2003).
37. O. Elgaroy and O. Lahav, New J. Physics, **7**, 61 (2005).
38. U. Seljak *et al.*, JCAP **0610**, 014 (2006).
39. P.T.P. Viana *et al.*, Mon. Not. Roy. Astr. Soc., **346**, 319 (2003).
40. S.D.M. White *et al.*, Nature **366**, 429 (1993).
41. P. Erdogdu *et al.*, Mon. Not. Roy. Astr. Soc. **340**, 573 (2003).
42. S.W. Allen *et al.*, Mon. Not. Roy. Astr. Soc. **342**, 287 (2003).
43. R.A.C. Croft *et al.*, Astrophys. J. **581**, 20 (2002).
44. S. Kim *et al.*, Mon. Not. Roy. Astr. Soc. **347**, 355 (2004).
45. U. Seljak *et al.*, Mon. Not. Roy. Astr. Soc. **342**, L79 (2003);
    U. Seljak *et al.*, Phys. Rev. D**71**, 103515 (2005).
46. P. Schneider, `astro-ph/0306465`;
    A. Refregier, Ann. Rev. Astron. Astrophys, **41**, 645 (2003).
47. H. Hoekstra *et al.*, Astrophys. J. **647**, 116 (2006).
48. A. Dekel, Ann. Rev. Astron. Astrophys. **32**, 371 (1994).
49. L. Silberman *et al.*, Astrophys. J. **557**, 102 (2001).
50. B. Chaboyer and L.M. Krauss, Science **299**, 65 (2003).
51. R. Cayrel *et al.*, Nature **409**, 691 (2001).
52. A. Blanchard *et al.*, Astron. Astrophys. **412**, 35 (2003).
53. C.J. MacTavish *et al.*, Astrophys. J. **647**, 833 (2006).